RoboWalk: Comprehensive Augmented Dynamics Modeling and performance analysis

S. A. A. Moosavian [a], M. Nabipour [a *]

a. Center of Excellence in Robotics and Control, Advanced Robotics & Automated Systems (ARAS) Lab, Department of Mechanical Engineering, K. N. Toosi University of Technology, Tehran, Iran

ARTICLE INFO

ABSTRACT

Utilizing orthosis and exoskeletons has drawn a lot of attention in many applications including medical industries. These devices are used in the area of physical therapy to facilitate the patient's exercises and as an assisting device to help the elderly carry out their daily activities. In this paper, the RoboWalk body-weight support assist device is introduced and its performance is analyzed by studying its influence on a human model. For this purpose, the forward kinematics of the human model and the inverse kinematics of RoboWalk are introduced in the first step. The dynamics of the human and a comprehensive model for RoboWalk are then obtained using the Newton-Euler method without considering the contact forces. These forces are then included in the model using the jacobian of contact points. The obtained models are then augmented to estimate the RoboWalk joint forces and torques, and those of the human model. The Recursive Newton Euler Algorithm and ADAMS software are used to verify the modeling obtained from the non-recursive Newton-Euler algorithm. The recursive algorithm is suitable for implementation purposes due to its low computational cost. After ensuring the accuracy of the obtained models, a control strategy is designed and implemented on RoboWalk. The performance of RoboWalk is then investigated by defining some criteria, e.g. floor reaction force and human model joint torques, before and after using RoboWalk.

1. Introduction

Orthosis and exoskeletons are devices used for curing people suffering from medical impairments by enabling the user to exercise the impaired limbs repeatedly. Another common field of application of such devices is the military for enhancing soldier strength. The Rehabilitation exoskeletons consist of two categories of treadmill-based immobile exoskeletons and mobile devices. The major difference between these categories is that in mobile devices treadmill isn't used and hence, the user walks with the device attached to it. In some cases, the user utilizes a walking stick to get help for maintaining stability. Robotic gait rehabilitation trainer[1], Lokomat[2], ALEX[3] and LOPES[4] are examples of treadmill-based devices. HAL[5], National University of Singapore orthosis[6], ReWalk[7] and etc. are some examples of portable rehabilitation devices.

The other main category of exoskeletons are strength augmentation and assistive systems. The first group is used in military armies and industries by a healthy subject to carry heavy weights for long period of time. The most famous exoskeleton of this kind is BLEEX[8] which is manufactured by University of California, Berkeley. Robo-Knee[9] and the MIT augmentation device[10] are other types of this category.

The assistive exoskeletons are mechanical devices that aim to reduce the physiological or metabolic cost during user's daily activities. They are classified into two groups of passive and active walking devices. Passive devices assist the user using elastic elements in their structure. The passive ankle exoskeleton[11], MoonWalker[12], XPED2[13], Bodyweight support device with compliant knee[14] and Ottawa passive device[15]. As for active assistive exoskeleton systems one can mention HULC[16], Honda's stride management [17] and bodyweight support device.

This paper lies in the continuity of previous works[18-20] done in the context of modeling, design and performance analysis of RoboWalk exoskeleton. After an introduction to RoboWalk compartments and its functionality, the kinematics of the user and RoboWalk is presented. In the next step, the human and the device are modeled by Newton-Euler's method. The modeling is performed in the sagittal plane and all the calculations are done in single support phase (SSP). The obtained models are then confirmed by modeling the human and the device using Adams software and Recursive Newton Euler Algorithm (RNEA). Then, a control strategy is proposed and the performance of this device under the function of this strategy is analyzed. The conclusions of this study are summarized in the last section.

2. Introducing RoboWalk

Figure 1 depicts the designed assistive robot (RoboWalk). This device comprises a pair of shoes, joints connecting the shoes to the expansion and contraction mechanism (lower frame and upper frame), a transmission mechanism, rails, bearings in the rails to transmit force from RoboWalk to the and a seat. Each rail is linked to one of the upper frames using two rollers. The only active joint in this robot is the knee actuator which is placed at the top rear part of the corresponding upper frame for the sake of ease of leg swinging motion. The torque of each motor is transferred to the RoboWalk knee joint by a transmission mechanism. The lower frames are connected to the shoes by a spherical joint. The user places its feet in the shoes. Then, the robot is turned on and the seat is raised until it is placed under the groin region of the human. The mechanism remains between the legs of the user in the entire gait. This design provides capability of maintaining the least moment of inertia during the gait. The rollers and guide rails of RoboWalk permit the hip joint to have 3-DOF. In addition, the knee joint is a 1-DOF joint in sagittal plane and the spherical joint used in the ankle provides a 3-DOF motion for user in the ankle. When the robot is in its standing position, the seat is stuck to user pelvis and therefore, its kinematics motion is related to user motion and specified uniquely.
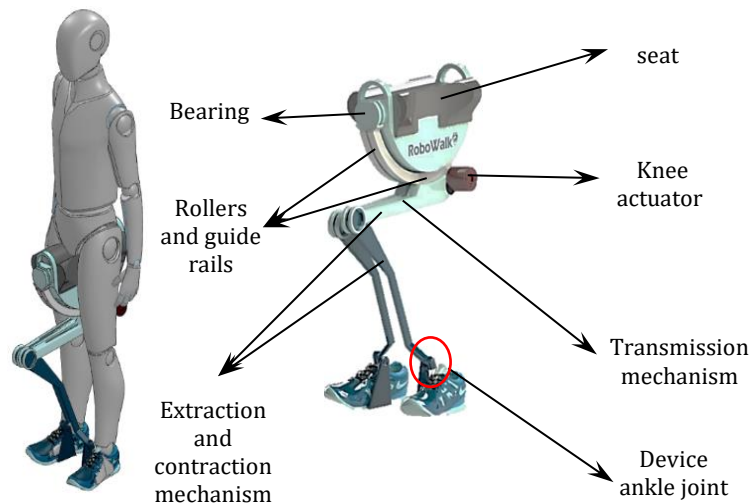

Figure 1. The CAD model of RoboWalk

3. Kinematic Modeling

In this section the kinematic model of both human and RoboWalk are discussed.

3.1. Human kinematic model

In this study, the human model consists of eight limbs and its movement is constrained in sagittal plane.

This model includes trunk, pelvis, left and right legs (i.e., foot, shank and thigh). All the upper limbs are substituted by the trunk for the sake of simplicity. The links are numbered from one to eight in a tree-structure topology by assuming the pelvis as the floating-base of the system. In order to formulize the kinematics of this system, a reference coordinate system is attached to the CoG of pelvis of the user. Pose and orientation of this coordinate is estimated with regard to the inertial

coordinate system placed on the ground as demonstrated in figure 2. Other coordinate system's alignment and position are defined regarding the floating-base coordinate.
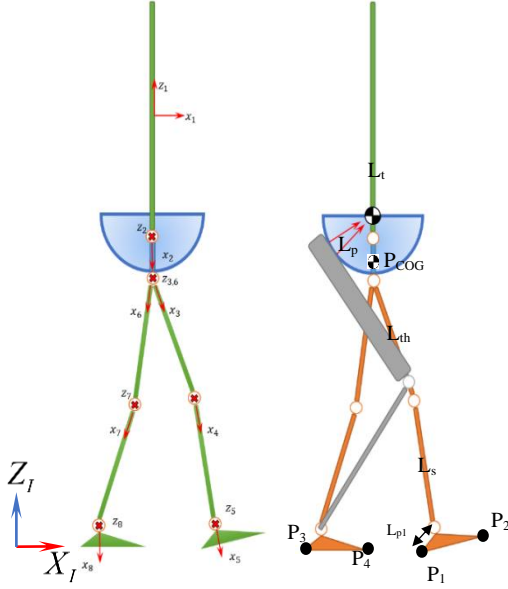

Figure 2. Coordinate frames on human and Schematic of human and robot.

A set of minimal generalized coordinates that define the motion of RoboWalk is stated as:

$$q = \begin{bmatrix} x_p & z_p & q_p & q_p & q_h & q_k & q_a \end{bmatrix}^T \quad (1)$$

where q_t, x_t and z_t are 1×3 vectors which define the motion of the pelvis reference coordinate regarding to stationary coordinate system. q_f, q_k, q_h and q_p represent the rotational motion of foot, knee, hip and pelvis joints regarding its parent limb. Since our study is performed in sagittal plane, these joint rotations represent a 1-DoF revolute joints and are all scalars. Hence, the human model is a 10-DoF kinematic tree structure.

Since the pelvis is chosen to be the floating base, the angle of rotation of other limbs are calculated by adding the successive angles from each parent to each child. In other words

$$q_{pelvis} = q_t + q_p$$

$$q_{hip} = q_t + q_p + q_h$$

$$q_{knee} = q_t + q_p + q_h + q_k \quad (2)$$

$$q_{ankle} = q_t + q_p + q_h + q_k + q_a$$

Since the kinematic data don't usually possess the x and z position (position of the floating-base with respect to the inertia), when obtaining the kinematics of human, they must be estimated. In order to estimate these positions numerically, the first step is to find the contacting part of the foot.

$$z_{t/p1} = L_t \cos q_t + L_p \cos q_{pelvis} + L_{th} \cos q_{hip}$$
$$+ L_s \cos q_{knee}$$
$$+ L_{p1} \cos(q_{ankle} + q_{p1})$$

$$x_{t/p1} = L_t \sin q_t + L_p \sin q_{pelvis} + L_{th} \sin q_{hip}$$
$$+ L_s \sin q_{knee}$$
$$+ L_{p1} \sin(q_{ankle} + q_{p1}) \quad (3)$$

Where, $z_{p/p1}$ and $x_{p/p1}$ represent the height and horizontal distance of pelvis CoG with regard to point p_1. L_t represents the length between top of pelvis and trunk CoG. L_{p1} is the distance between the ankle and p_1. L_p, L_{th} and L_s represent the pelvis, thigh and shank lengths, respectively. $z_{p/p2}$, $z_{p/p3}$, $z_{p/p4}$, $x_{p/p2}$, $x_{p/p3}$ and $x_{p/p4}$ are written correspondingly. derivative of the mentioned relative positions are calculated by differentiating them with respect to time.

Height of floating-base with respect to the ground (z_t) is obtained by the following.

$$z_p = max(z_{p/p1}. z_{p/p2}. z_{p/p3}. z_{p/p4}) \quad (4)$$

This equation specified the foot point of contact. This point is also used to define the horizontal position of the floating-base regarding the inertial coordinate.

$$x_p(i) = x_p(i-1) + \dot{x}_p(i-1) \times \Delta t \quad (5)$$

where Δt is the sampling time. The horizontal and vertical velocity of the floating-base is calculated using the contact point (by assuming that p_1 is the contact point):

$$\dot{x}_p = \dot{x}_{p/p1} \ , \ \ddot{x}_p = \ddot{x}_{p/p1}$$
$$\dot{z}_p = \dot{z}_{p/p1} \ , \ \ddot{z}_p = \ddot{z}_{p/p1} \quad (6)$$

It is assumed that the seat and the rails are stuck to human pelvis, hence, the seat's pose is the same as the pose of human pelvis. Another assumption is made for simplicity of modeling the human-robot interaction. In this regard it is supposed that the shoes are a part of user foot and any force applied by the robot through lower frames are directly exerted to human foot (figure 2).

3.2. RoboWalk kinematic model:

$\overrightarrow{F_1}$ and $\overrightarrow{F_2}$ are the forces exerted to the human by RoboWalk through the seat. These forces are generated because of the contact between the rollers and the seat, hence they are perpendicular to the arc guides and their direction is toward the approximate CoG of the user (friction is neglected). The direction of $\overrightarrow{F_1}$ and $\overrightarrow{F_2}$ can be obtained by kinematic approaches. One can think of the lower frame, upper frame and the distance between the rollers and human's COG (the arc's radius) as links of a 3-link robot. This concept is shown in Fig. 3.
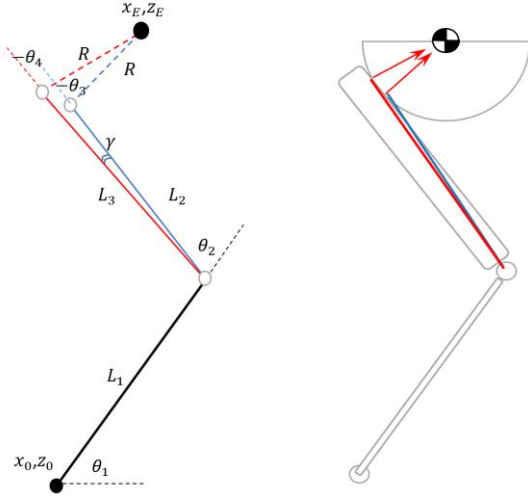
Figure 3. Finding assistance force directions and RoboWalk kinematics.

Where L_2 and L_3 are the length between the robot's knee joint and first and second roller, respectively. R is the seat's arc radius (which is assumed to be the third hypothetical link). (x_0, z_0) and (x_e, z_e) are the positions of the ankle of robot and the human's COG in inertial coordinate frame, respectively. In this approach, if the orientation of both hypothetical links were obtained, the orientation of forces $\vec{F_1}$ and $\vec{F_2}$ is resulted. Hence, by solving the inverse kinematics of two 3-link robot at once, the orientation of $\vec{F_1}$ and $\vec{F_2}$ are obtained. (7) and (8) show the forward kinematics for the first 3-link robot (consisting of L_1, L_2 and R):

$$x_E - x_0 = L_1 cos\theta_1 + L_2 \cos(\theta_1 + \theta_2) \\ + Rcos(\theta_1 + \theta_2 + \theta_3) \qquad (7)$$

$$z_E - z_0 = L_1 sin\theta_1 + L_2 \sin(\theta_1 + \theta_2) \\ + Rsin(\theta_1 + \theta_2 + \theta_3) \qquad (8)$$

In this equation, θ_1 is the angular displacement of L_1 from horizontal line. θ_2 is the angular displacement of L_2 with respect to L_1 and θ_3 is the angular displacement of R with respect to L_2. The inverse kinematics problem for the second 3-link robot (consisting of L_1, L_3 and R) is obtained as:

$$x_E - x_0 = L_1 cos\theta_1 + L_3 \cos(\theta_1 + \theta_2 + \gamma) \\ + Rcos(\theta_1 + \theta_2 + \gamma + \theta_4) \qquad (9)$$

$$z_E - z_0 = L_1 sin\theta_1 + L_3 \sin(\theta_1 + \theta_2 + \gamma) \\ + Rsin(\theta_1 + \theta_2 + \gamma + \theta_4) \qquad (10)$$

Where γ is the angular difference between L_2 and L_3 and θ_4 is the angular displacement of L_3 with respect to L_1. By solving these four equation numerically for each time step, the four unknowns ($\theta_1, \theta_2, \theta_3$ and θ_4) are obtained. θ_1 and θ_2 are the angle of the contraction and expansion mechanism and θ_3 and θ_4 are equal to the direction of the forces $\vec{F_1}$ and $\vec{F_2}$.

4. Dynamics Modeling:

In this section, we aim to develop dynamics model for a human and the assistive robot having general interaction with environment. In order to state the set of equation of motion in a valid form for all phases, first, the human is considered as free body without any interaction with environment. The set of unconstrained equations can be stated as[19]:

$$M(q)\ddot{q} + V(q.\dot{q}) + G(q) = B\tau \qquad (11)$$

Where M is a (10×10) matrix. Also, V, G and $B\tau$ are vectors with (10×1) elements. Left hand side of is composed of inertia effects, Coriolis and centrifugal and gyration, and gravity effects. $B\tau$ represents generalized forces acting on the robot and is different during various phases of motion and B is a 7×10 matrix presented by:

$$B = [0_{7\times3} \ \ I_{7\times7}]^T \qquad (12)$$

And vector τ is defined as:

$$\tau = \begin{bmatrix} 0_{1\times3} & \tau_p & \tau_{rh} & \tau_{rk} & \tau_{ra} & \tau_{lh} & \tau_{lk} & \tau_{la} \end{bmatrix}^T \qquad (13)$$

Which τ_p, τ_{rh}, τ_{rh}, τ_{rk}, τ_{ra}, τ_{lh}, τ_{lk} and τ_{la} are pelvis, right and left hip, knee and ankle joint torques, respectively. There are various methods to obtain the dynamics equation mentioned in (11) such as Lagrange, Newton and Newton-Euler (NE) algorithms. One of the most notable properties of Lagrange formulation is the capacity to eliminate all internal reaction forces of the system from the final equation of motion (EoM), in contrast to the Newton and Newton-Euler formulation where there they are explicitly accounted for. Since one of the future goals of our project is to minimize the forces in certain joints in human body, Newton and NE techniques were used for obtaining the EoM.

In order to obtain an equation similar to (11), all internal reaction forces must be eliminated. Hence, by substituting the amount of these forces by their kinematic values, the EoM is obtained as (11). In order to develop constrained dynamics model, this constraint is replaced by unknown forces and moments acting on a point on the foot sole. Then, using transpose of jacobian of point of contact, these forces and moments are mapped to the space of generalized coordinates. As a result, the equations of motion in the case of SSP is specified as:

$$M(q)\ddot{q} + V(q.\dot{q}) + G(q) = B\tau + J^T F \qquad (12)$$

Where:

$$F = \begin{bmatrix} F_{contact} \\ M_{contact} \end{bmatrix} \qquad (13)$$

The unknown forces are obtained by:

$$\begin{bmatrix} \tau \\ F \end{bmatrix}_{10\times1} = [B \quad J^T]^{-1}_{10\times10}[M(q)\ddot{q} + V(q.\dot{q}) \\ + G(q)] \qquad (14)$$

When the user utilizes the RoboWalk, the EoM in SSP changes into

$$\begin{bmatrix} \tau \\ F \end{bmatrix}_{10\times1} = [B \quad J^T]^{-1}_{10\times10}[M(q)\ddot{q} + V(q.\dot{q}) \\ + G(q) - J_{LA}^T F_{LA} - J_{RA}^T F_{RA} \\ - J_{COG}F_{COG}] \tag{15}$$

In this equation, J_{LA}, J_{RA} and J_{COG} represent the jacobian of robot left and right ankle that are connected to the user's shoe and the jacobian of user's COG. F_{LA}, F_{RA} and F_{COG} are known forces acting on those positions. Hence, in SSP τ and F are uniquely specified. If the human is in double support phase (DSP) the EoM is changed into

$$M(q)\ddot{q} + V(q.\dot{q}) + G(q) = B\tau + J_L^T F_L + J_R^T F_R \tag{16}$$

Where J_L and J_R are the jacobian of the left and right foot contact point, and F_L and F_R are the contact forces of left and right foots, respectively. Because the number of unknown parameters in DSP is larger than the number of equations, there is more than one answer for dynamic model in this phase. So that, pseudo inverse is used for solving the dynamic equations to obtain minimum norm answer. Pseudo inverse of an arbitrary matrix A is as follow:

$$A^+ = A(A^T A)^{-1} \tag{17}$$

In the next step, the exoskeleton is modeled by the Newton's technique. In order to do so, the free-body and kinetic diagram of the links of the robot is shown in Fig. 5. Since the equations for both sides are the same, only one of robot's feet is shown.
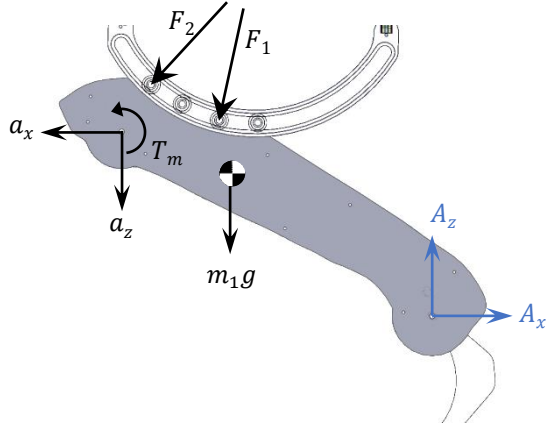

Figure 4. FBD of RoboWalk upper link.

In this figure, $\overrightarrow{F_1}$ and $\overrightarrow{F_2}$ are forces applied to the robot seat through the upper frames by the two rollers in the seat's slider. Since the rollers only apply normal forces, the only interaction between the robot seat and human body is modeled by F_1 and F_2. A_x, A_z and M are internal forces and motor torque exerted on the robot's knee joint, respectively.

$$X : A_x - a_x - F_1 \cos\alpha_{f_1} - F_2 \cos\alpha_{f_2} = m_1 \ddot{x}_{G_1} \\ Z : A_z - a_z - m_1 g - F_1 \sin\alpha_{f_1} - F_2 \sin\alpha_{f_2} = m_1 \ddot{z}_{G_1} \tag{18}$$

$$\sum M_{CoG} : T_m + a_z x_m - a_x z_m + A_z L \sin\theta_1 \\ + A_x L \cos\theta_1 + m_1 ga = I_{G_1}\ddot{\theta}_1 + m_1\left(b\ddot{x}_{G_1} - a\ddot{z}_{G_1}\right) \tag{19}$$

where

$$x_m = L_m \sin\left(\theta_1 + \alpha_0\right) - L\sin\theta_1 \\ z_m = L\cos\theta_1 - L_m \cos\left(\theta_1 + \alpha_0\right) \\ a = L_{G_1}\sin\left(\theta_1 + \alpha_0\right) - L\sin\theta_1 \\ b = L\cos\theta_1 - L_{G_1}\cos\left(\theta_1 + \alpha_0\right) \tag{20}$$

the CoG of human which is assumed to be the center of arc rails. θ_1 and θ_2 are upper and lower frame angles with respect to vertical, respectively.
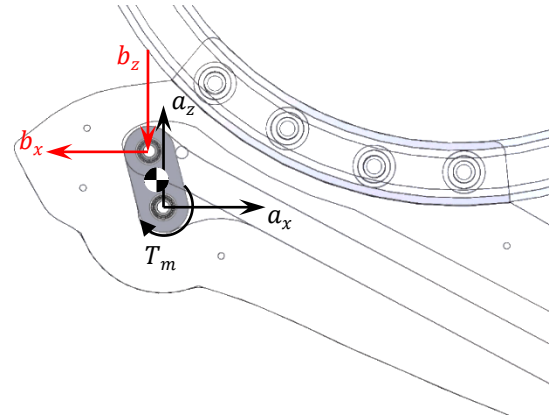

Figure 5. FBD of link (a) of transmission mechanism.

$$X : a_x - b_x = m_a \ddot{x}_a \\ Z : a_z - b_z - m_a g = m_a \ddot{z}_{G_a} \tag{21}$$

$$\sum M_a : -T_m - m_a g \frac{L_a}{2}\cos\theta_a + b_x L_a \sin\theta_a \\ - b_z L_a \cos\theta_a = I_a \ddot{\theta}_a + m_a \frac{L_a}{2}\left(-\ddot{x}_a \sin\theta_a + \ddot{z}_a \cos\theta_a\right) \tag{22}$$
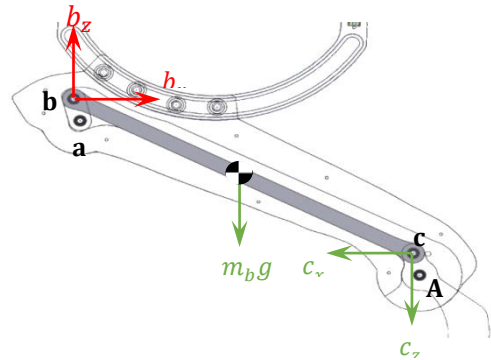

Figure 6. FBD of link (b) of transmission mechanism.

$$X : b_x - c_x = m_b \ddot{x}_b$$
$$Z : b_z - c_z - m_b g = m_b \ddot{z}_{G_b}$$
(23)

$$\sum M_b : c_x L_b \sin\theta_b - L_b \cos\theta_b \left(c_z + \frac{m_b g}{2} \right)$$
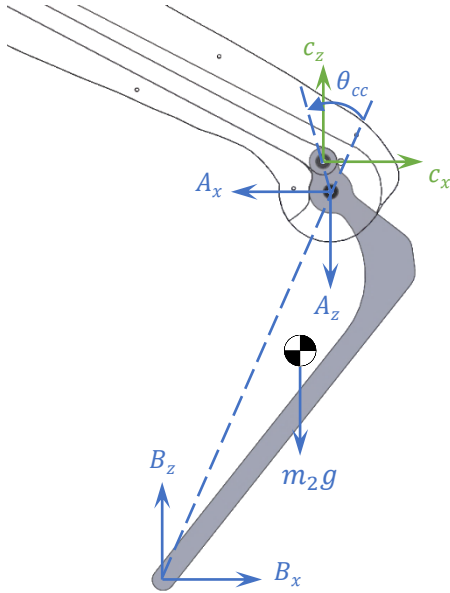$$= I_b \ddot{\theta}_b + m_b \frac{L_b}{2} \left(-\ddot{x}_b \sin\theta_b + \ddot{z}_b \cos\theta_b \right)$$
(24)

Figure 7. FBD of RoboWalk lower link.

$$X : B_x + c_x - A_x = m_2 \ddot{x}_{G_1}$$
$$Z : B_z + c_z - A_z - m_2 g = m_2 \ddot{z}_{G_2}$$
(25)

$$\sum M_A : B_x r \cos(\theta_1 + \theta_2) + B_z r \sin(\theta_1 + \theta_2)$$
$$-m_2 g r_{G2} \sin(\theta_1 + \theta_2 + \beta) - c_z L_c \sin(\theta_1 + \theta_2 + \theta_{cc})$$
$$-c_x L_c \cos(\theta_1 + \theta_2 + \theta_{cc}) =$$
$$I_{G2}(\ddot{\theta}_1 + \ddot{\theta}_2) + m_2 \ddot{x}_{G2} r_{G2} \cos(\theta_1 + \theta_2 + \beta)$$
$$+m_2 \ddot{z}_{G2} r_{G2} \sin(\theta_1 + \theta_2 + \beta)$$
(26)

where B_x and B_z are forces exerted by the spherical joint to ankle of the robot. As a result of these equations, there are 12 equations for each RoboWalk leg.

Since the directions of $\overrightarrow{F_1}$ and $\overrightarrow{F_2}$ is known by knowing the kinematics, there exists 13 unknowns, e.g. $\overrightarrow{F_1}, \overrightarrow{F_2}, T_m, a_x, a_z, b_x, b_z, c_x, c_z, A_x. A_z, B_x$ and B_z.

As stated before, our goal is to compensate 33% of user's weight. The only way for the robot to assist the user (apply force to user) is through the seat. Hence, the resultant vertical force applied to human by the robot should be equal to 33% of the user's bodyweight. This notion is illustrated in (27) as follow.

$$F_{1_z} + F_{2_z} = pW$$
(27)

Where W is the weight of the user and p is a number between 0 and 1 (1/3 in this case study). By obtaining this equation, the number of equations are equal to the number of unknowns and the dynamics is completely solvable.

Another approach to model the human motion is using the Recursive Newton Euler Algorithm (RNEA). This algorithm uses NE algorithm and solves the problem by 6×1 spatial coordinates instead of 3×1 common representations (Refer to [21] for more details). In Fig. 4 the free body diagram of body i is shown.
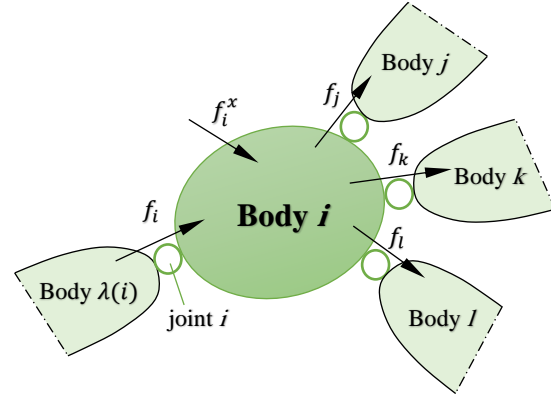

Figure 8. Forces acting on body (i)

In this figure, $\lambda(i)$ is the parent, f_i is the force exerted by the parent to body i, f_i^x is the external force exerted on body i. They are regarded as inputs to the algorithm; that is, their values are assumed to be known. Other forces are the forces exerted by body i to the children bodies.

The spatial equation of motion states that the net force acting on a rigid body equals its rate of change of momentum:

$$f_i^B = \frac{d}{dt}(I_i v_i) = I_i a_i + v_i \times^* I_i v_i$$
(28)

Where $\times^*$ is spatial force product, v_i, a_i and I_i are spatial velocity, acceleration and inertia respectively and f_i^B is the net force acting on body i. it can be concluded from Fig. 4 that:

$$f_i^B = f_i + f_i^x - \sum_{j \in \mu(i)} f_j$$
(29)

which can be rearranged to give a recurrence relation for the joint forces:

$$f_i = f_i^B - f_i^x + \sum_{j \in \mu(i)} f_j$$
(30)

non-recursive algorithms calculated the dynamics via equations like (11), and their computational complexities were typically $O(n^4)$[22]. Recursive algorithms are far more efficient, and they have computational complexities as low as $O(n)$.

Since our algorithms are going to be implemented on the exoskeleton and the inverse dynamics problem must be solved every few milliseconds, and solving this problem analytically is time consuming, using recursive Newton-Euler algorithm in implementation is preferred.

5. Results and Discussion:

In this section the dynamics of the 10 DOF human and the 6 DOF assistive lower limb robot is developed and the results for a specified walking pattern will be discussed and evaluated. The kinematics of the entire system is verified in figure 9.

In this figure, the gait data is extracted from Opensim software. As it is shown, the human kinematics seems natural and the robot and its mechanism follows the human user properly.

Because of number of degrees of freedom of the human and RoboWalk, the procedure of dynamics modeling is error prone and model verification should be carried out. In order to verify the dynamics model, three analytical and numerical methods i.e. Newton's method, ADAMS software and RNEA, are exploited.
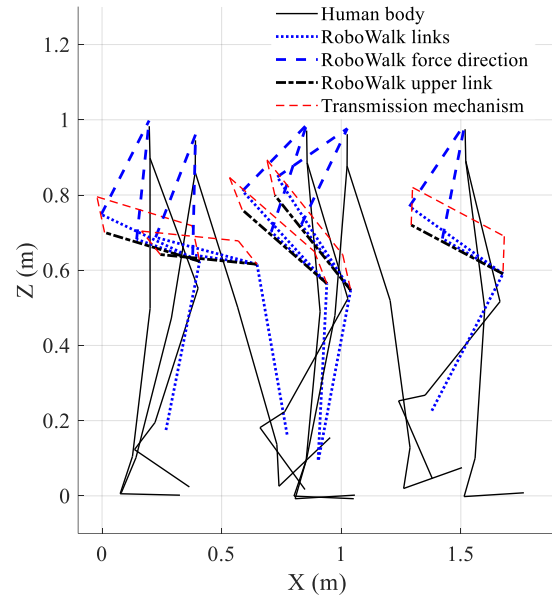

Figure 9. Verification of human model and RoboWalk kinematics

Sinusoidal trajectories are applied to the joints and obtained results from two models are compared in figure 10.
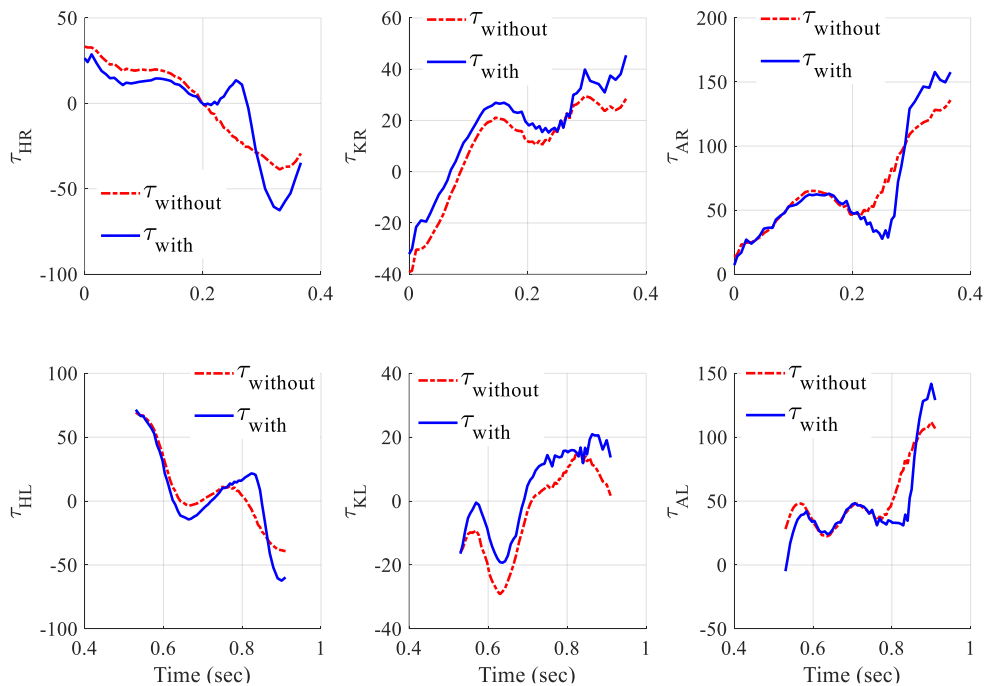

FIGURE 10.. Human joint forces and torques with and without RoboWalk

69

(a) Dynamics verification by RNEA method

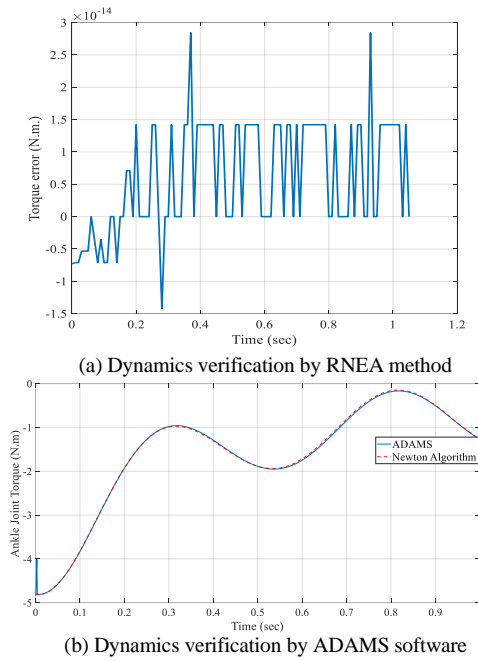(b) Dynamics verification by ADAMS software

Figure 11. Verification of dynamics model (a) by RNEA method, (b) by ADAMS software

As it can be observed from this figure, both methods yield same results and the error between them in RNEA method is of the order of 10^{-14} , which is due to computation round off. Also, it seems necessary to mention that the sinusoidal trajectories that are applied to the joints do not result feasible motion for the robot and just considered to apply a wide range of values to the joints. In Table I and II the human and RoboWalk's mass and geometric properties are illustrated.

Table 1. Mass properties of the human

Link	Mass (Kg)
Foot	0.82
Shank	2.64
Thigh	5.67
Pelvis	8.05
Trunk	30.39
Upper link mass	3
Lower link mass	1
Human total weight	56.7
Robot total weight	8

Table 2. Geometric properties of the human and RoboWalk

Link	Length (m)
Foot length	0.25
Ankle joint height	0.05
Shank	0.4
Thigh	0.4
Pelvis	0.1
Trunk	0.8
Robot upper link length	0.55
Robot lower link length	0.55
Horizontal distance between robot ankle and human ankle	0.05
Vertical distance between robot ankle and human ankle	0
Circle arc radius	0.25

By substituting joints trajectories from Opensim into the dynamics model, joints torques are computed. The assistive method of the robot that we used is that whenever a leg of the human is in its stance phase, the robot will assist the person (the actuator is ON) and when the leg is in its swing phase the actuator gets OFF. In figure 11 forces and torques of human Joints and in figure 12 the FRF of the left foot of the user, in SSP, with and without using RoboWalk is illustrated.
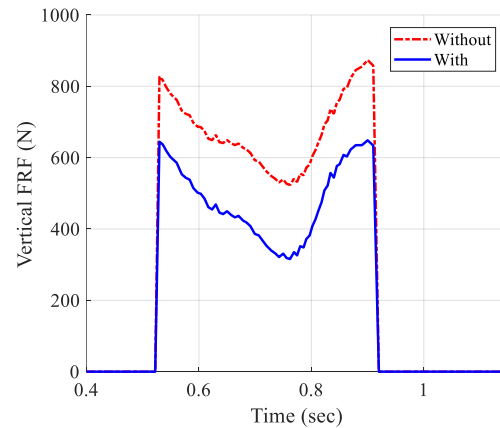

Figure 12. FRF of the user

As stated before, the FRF eliminates the forces and torque of the virtual joint in the pelvis. It is seen that almost 33% of the FRF is compensated.

In Fig. 11, the red-dashed lines are the user's joint torques without using RoboWalk. The blue-solid lines are the joint torques after the user wear the robot. T_H, T_K and T_A represent hip, knee and ankle torques

respectively. As illustrated if this figure, after using the robot, the joint torques of the stance leg (left leg) has decreased significantly in most of the gait cycle. The robot motor torque that caused this reduction in user joint torques is given in figure 13 as follow.
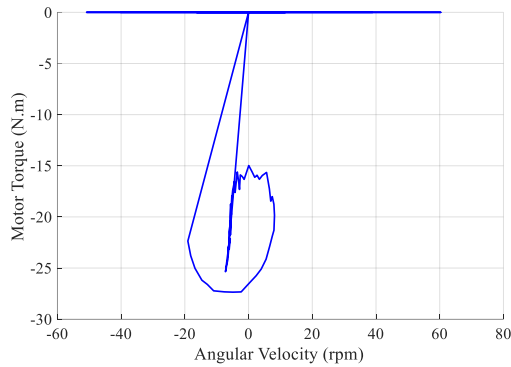

Figure 13.Robot's left motor torque-speed curve

Considering this figure, in order to achieve the goal of our control strategy for compensating 33% of user's bodyweight the actuator of the device should be able to provide approximately 25 N.m torque in maximum velocity of 20 rpm.

6. Conclusion

In this research, an assistive lower limb exoskeleton, RoboWalk, was introduced and its functionality and operational strategy was expressed. This exoskeleton was kinematically and dynamically modeled in the next step. The obtained model was a comprehensive model in sagittal plane which includes the modeling of the transmission mechanism of the actuating system. The verification was performed using two methods of modeling the system by RNEA method and ADAMS software. A control strategy was then designed and applied to RoboWalk model to investigate the device's performance and its effect on user. The results showed that the robot reduces the felt bodyweight (the floor reaction force) of the user by 33% using a 25 N.m. motor in maximum 20 rpm angular velocity. The obtained range for the motor gives us a lot of choices for selecting an appropriate actuating system for RoboWalk. It should be mentioned that for the sake of safety, the actuating system must be back-drivable. Which makes Maxon motor flat motors (e.g. EC 90 flat Ø90 mm, 360 W) a very ideal choice for this system. In addition, in the analyzes, the knee joint force was chosen as a criterion to analyze the comfort of the user. The results showed a reduction in joint torques of the user in most of the gait. The next step of this research is finding a solution to increase RoboWalk effect on the remaining parts of the user gait.

References

[1] M. Pietrusinski, I. Cajigas, G. Severini, P. Bonato, and C. Mavroidis, "Robotic gait rehabilitation trainer," *IEEE/ASME Transactions On Mechatronics,* vol. 19, no. 2, pp. 490-499, 2013.

[2] G. Colombo, M. Joerg, R. Schreier, and V. Dietz, "Treadmill training of paraplegic patients using a robotic orthosis," *Journal of rehabilitation research and development,* vol. 37, no. 6, pp. 693-700, 2000.

[3] S. K. Banala, S. H. Kim, S. K. Agrawal, and J. P. Scholz, "Robot assisted gait training with active leg exoskeleton (ALEX)," in *2008 2nd IEEE RAS & EMBS International Conference on Biomedical Robotics and Biomechatronics*, 2008, pp. 653-658: IEEE.

[4] J. F. Veneman, R. Kruidhof, E. E. Hekman, R. Ekkelenkamp, E. H. Van Asseldonk, and H. Van Der Kooij, "Design and evaluation of the LOPES exoskeleton robot for interactive gait rehabilitation," *IEEE Transactions on Neural Systems and Rehabilitation Engineering,* vol. 15, no. 3, pp. 379-386, 2007.

[5] H. Kawamoto and Y. Sankai, "Power assist system HAL-3 for gait disorder person," in *International Conference on Computers for Handicapped Persons*, 2002, pp. 196-203: Springer.

[6] G. Chen, P. Qi, Z. Guo, and H. Yu, "Mechanical design and evaluation of a compact portable knee–ankle–foot robot for gait rehabilitation," *Mechanism and Machine Theory,* vol. 103, pp. 51-64, 2016.

[7] I. Díaz, J. J. Gil, and E. Sánchez, "Lower-limb robotic rehabilitation: literature review and challenges," *Journal of Robotics,* vol. 2011, 2011.

[8] A. B. Zoss, H. Kazerooni, and A. Chu, "Biomechanical design of the Berkeley lower extremity exoskeleton (BLEEX)," *IEEE/ASME Transactions on mechatronics,* vol. 11, no. 2, pp. 128-138, 2006.

[9] J. E. Pratt, B. T. Krupp, C. J. Morse, and S. H. Collins, "The RoboKnee: an exoskeleton for enhancing strength and endurance during walking," in *IEEE International Conference on Robotics and Automation, 2004. Proceedings. ICRA'04. 2004*, 2004, vol. 3, pp. 2430-2435: IEEE.

[10] C. J. Walsh, K. Endo, and H. Herr, "A quasi-passive leg exoskeleton for load-carrying augmentation," *International Journal of Humanoid Robotics,* vol. 4, no. 03, pp. 487-506, 2007.

[11] S. H. Collins, M. B. Wiggin, and G. S. Sawicki, "Reducing the energy cost of human walking

using an unpowered exoskeleton," *Nature,* vol. 522, no. 7555, p. 212, 2015.

[12] W. van Dijk and H. Van der Kooij, "XPED2: A passive exoskeleton with artificial tendons," *IEEE robotics & automation magazine,* vol. 21, no. 4, pp. 56-61, 2014.

[13] S. Krut, M. Benoit, E. Dombre, and F. Pierrot, "Moonwalker, a lower limb exoskeleton able to sustain bodyweight using a passive force balancer," in *2010 IEEE International Conference on Robotics and Automation*, 2010, pp. 2215-2220: IEEE.

[14] K.-M. Lee and D. Wang, "Design analysis of a passive weight-support lower-extremity-exoskeleton with compliant knee-joint," in *2015 IEEE International Conference on Robotics and Automation (ICRA)*, 2015, pp. 5572-5577: IEEE.

[15] Z. Lovrenovic, "Development and Testing of Passive Walking Assistive Exoskeleton with Upward Force Assist," Université d'Ottawa/University of Ottawa, 2017.

[16] C. Buesing *et al.*, "Effects of a wearable exoskeleton stride management assist system (SMA®) on spatiotemporal gait characteristics in individuals after stroke: a randomized controlled trial," *Journal of neuroengineering and rehabilitation,* vol. 12, no. 1, p. 69, 2015.

[17] Y. Ikeuchi, J. Ashihara, Y. Hiki, H. Kudoh, and T. Noda, "Walking assist device with bodyweight support system," in *2009 IEEE/RSJ International Conference on Intelligent Robots and Systems*, 2009, pp. 4073-4079: IEEE.

[18] S. A. A. Moosavian, M. R. Mohamadi, and F. Absalan, "Augmented Modeling of a Lower Limb Assistant Robot and Human Body," in *2018 6th RSI International Conference on Robotics and Mechatronics (IcRoM)*, 2018, pp. 337-342: IEEE.

[19] M. Nabipour and S. A. A. Moosavian, "Dynamics Modeling and Performance Analysis of RoboWalk," in *2018 6th RSI International Conference on Robotics and Mechatronics (IcRoM)*, 2018, pp. 445-450: IEEE.

[20] A. A. M. Nasrabadi, F. Absalan, and S. A. A. Moosavian, "Design, kinematics and dynamics modeling of a lower-limb walking assistant robot," in *2016 4th International Conference on Robotics and Mechatronics (ICROM)*, 2016, pp. 319-324.

[21] B. Siciliano and O. Khatib, *Springer handbook of robotics*. Springer, 2016.

[22] R. Featherstone, *Rigid body dynamics algorithms*. Springer, 2014.

7. Biography

S. Ali A. Moosavian received his B.S. degree in 1986 from Sharif University of Technology, and M.S. degree in 1990 from Tarbiat Modaress University (both in Tehran), and a Ph.D. degree in 1996 from McGill Univ. (Montreal, Canada), all in Mechanical Engineering. He is currently a Professor of the Mechanical Eng Dept at

K. N. Toosi University of Technology (Tehran). He teaches courses in the areas of robotics, dynamics, automatic control, analysis and synthesis of mechanisms. His current research interests include the area of robotics, modeling and control of dynamic systems, and mechatronics and designs. He has published more than 300 articles in journals and conference proceedings. He is one of three founders of the ARAS Research Center for Design, Manufacturing and Control of Robotic Systems, and Automatic Machineries.

Mahdi Nabipour received his B.S. degree in 2011 from

Shahid Chamran University of Ahvaz, and M.S. degree in 2014 from Amirkabir University of Technology in Tehran. He is currently a Ph.D. candidate of Mechanical Engineering in K. N. Toosi University of Technology. His research interest is in the area of rehabilitation, assistive robotics and aerospace engineering.